

Longitudinal Control of a Platoon of Vehicles with no Communication of Lead Vehicle Information: A System Level Study

Shahab Sheikholeslam and Charles A. Desoer, *Fellow, IEEE*

Abstract—This paper considers the problem of longitudinal control of a platoon of automotive vehicles on a straight lane of a highway and proposes control laws in the event of loss of communication between the lead vehicle and the other vehicles in the platoon. After discussing the main design objectives for the proposed control laws, we formulate these objectives as a constrained optimization problem. By solving this optimization problem, we obtain longitudinal control laws for a platoon of vehicles which does not use any communication from the lead vehicle to the other vehicles in the platoon. Comparison between these control laws and the control laws which use such a communication link to transmit lead-vehicle information to the other vehicles in a platoon shows that, in the case of loss of communication between the lead vehicle and the other vehicles, the performance of the longitudinal control laws degrades; however, this degradation is not catastrophic.

I. INTRODUCTION

TRAFFIC congestion is a global problem. One method to increase traffic flow is to decrease inter-vehicle spacings, thus forming a platoon of vehicles traveling at high speed. One way to achieve this objective is to control automatically the dynamics of vehicles within a platoon. The concept of an automatically-controlled platoon of vehicles with the corresponding sensor, actuator, and communication requirements is discussed in [15], [16] and references therein. Much work has been done in the study of longitudinal control of a platoon of vehicles on automated guideway transit systems [2]–[5], [7], [9], [14], [15]. The problem of longitudinal control of longer platoons of *nonidentical* vehicles was presented in [11] and [12]. A platoon consists of a lead vehicle followed by vehicles 1, 2, ..., N .

In [11] and [12], longitudinal control laws for each vehicle in the platoon, say the i th vehicle, use the lead vehicle's velocity (v_l) and acceleration (a_l) in addition to the preceding vehicle's velocity (v_{i-1}), acceleration (a_{i-1}), and the distance between vehicle i and the preceding vehicle, $i - 1$. In these papers, the lead vehicle's velocity (v_l) and acceleration (a_l) are transmitted to each vehicle in the platoon via a communication link. From a system point of view, an important question is: what is the loss of performance if communication from the lead vehicle to other vehicles is lost? The purpose of this

paper is to evaluate the performance of longitudinal control laws with *no communication of lead vehicle information*.

The organization of this paper is as follows: in Section II, after giving a brief review of vehicle model and exact linearization and normalization of vehicle dynamics [11], [12], we propose a longitudinal control law which uses no lead vehicle information and present the resulting platoon dynamics; in Section III, we present design considerations for the proposed control laws and formulate these considerations as an optimization problem; in Section IV, we present the simulation results for a platoon of vehicles under the control laws obtained by solving the above optimization problem and compare the performance of these laws with those which require communication of lead vehicle information [11], [12]; in Section V, we discuss some of the trade-offs involved in using the proposed control laws. An abbreviated version of this paper appeared in [13].

II. PROPOSED CONTROL LAWS AND PLATOON DYNAMICS

In this section, we review the vehicle model and the exact linearization of vehicles' longitudinal dynamics [11], [12]. Then, we propose longitudinal control laws which do not require communication of the lead vehicle's velocity (v_l) and acceleration (a_l) to each vehicle in the platoon. Using the proposed control laws, we obtain a block diagram for analyzing the platoon dynamics.

We consider a platoon of N vehicles following a lead vehicle on a straight lane of highway [11], [12] (see Fig. 1): each vehicle in the platoon is assigned a slot of length L ; the abscissa of the rear bumper of the i th vehicle with respect to a fixed point O on the road is denoted by x_i ; for $i = 1, 2, \dots, N$, Δ_i denotes the deviation of the i th vehicle's position from its assigned position. Hence, we have

$$\Delta_1 := x_1 - x_1 - L$$

and for $i = 2, 3, \dots, N$,

$$\Delta_i := x_{i-1} - x_i - L.$$

A. Vehicle Model [11], [12]

The longitudinal dynamics of the i th vehicle in the platoon are modeled as follows (for $i = 1, 2, \dots, N$):

$$\dot{F}_i = -\frac{F_i}{\tau_i(\dot{x}_i)} + \frac{u_i}{\tau_i(\dot{x}_i)} \quad (1)$$

Manuscript received September 1992; revised October 1993. This work was supported in part by the PATH Project, under Grant RTA-74H221, and by the National Science Foundation under Grant NSF-88-05767.

The authors are with the Department of Electrical Engineering and Computer Science, University of California at Berkeley, Berkeley, California 94720.

IEEE Log Number 9209423.

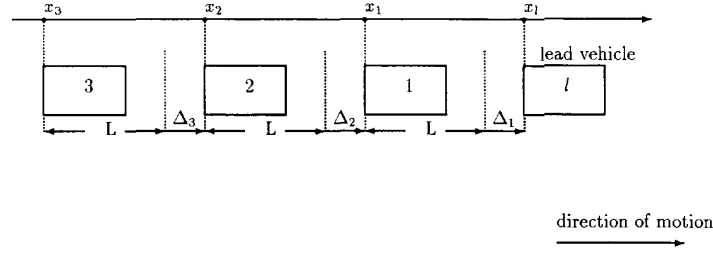


Fig. 1. A platoon of vehicles on a straight lane of highway.

$$m_i \ddot{x}_i = F_i - K_{di} \dot{x}_i^2 - k_{mi} \quad (2)$$

where F_i denotes the driving force produced by the i th vehicle's engine; m_i denotes the mass of the i th vehicle; $\tau_i(\cdot)$ denotes the engine time lag for the i th vehicle; u_i denotes the throttle command input to the i th vehicle's engine; K_{di} denotes the aerodynamic drag coefficient for the i th vehicle; and d_{mi} denotes the i th vehicle's mechanical drag. Equation (1) represents the i th vehicle's engine dynamics, and (2) represents Newton's second law applied to the i th vehicle modelled as a particle of mass m_i .

This simple model used to describe the engine dynamics (1) has proved to be useful for preliminary system level studies in longitudinal control of a platoon of vehicles [2], [3], [14], [15].

B. Exact Linearization of Vehicle Longitudinal Dynamics [11], [12]

In the sequel, we use exact linearization methods [8], [10] to *linearize* and *normalize* the input-output behavior of each vehicle in the platoon. Differentiating both sides of (2) with respect to time and substituting the expression for \ddot{F}_i in terms of \dot{x}_i and \ddot{x}_i from (1), (2) we obtain (for $i = 1, 2, \dots, N$):

$$\ddot{x}_i = b_i(\dot{x}_i, \ddot{x}_i) + a_i(\dot{x}_i)u_i \quad (3)$$

where

$$b_i(\dot{x}_i, \ddot{x}_i) = -\frac{1}{\tau_i(\dot{x}_i)} \left[\ddot{x}_i + \frac{K_{di}}{m_i} \dot{x}_i^2 + \frac{d_{mi}}{m_i} \right] - \frac{2K_{di}}{m_i} \dot{x}_i \ddot{x}_i \quad (4)$$

and

$$a_i(\dot{x}_i) = \frac{1}{m_i \tau_i(\dot{x}_i)}. \quad (5)$$

We propose the following control law (for $i = 1, 2, \dots, N$):

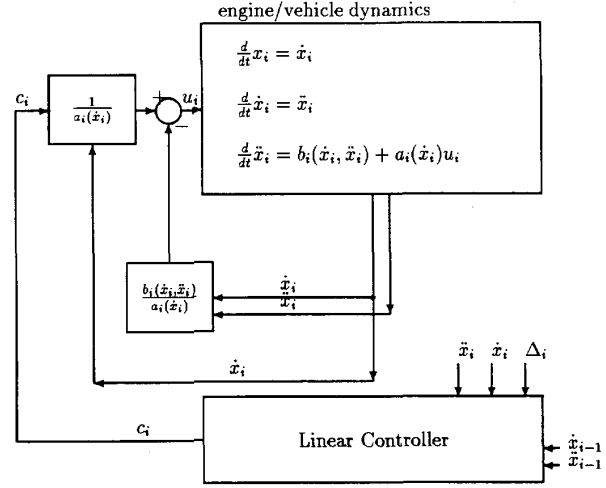
$$u_i(\dot{x}_i, \ddot{x}_i) = \frac{1}{a_i(\dot{x}_i)} [-b_i(\dot{x}_i, \ddot{x}_i) + c_i] \quad (6)$$

where c_i is an exogenous input to the i th vehicle dynamics.

Substituting the expression for u_i from (6) into (3) we obtain (for $i = 1, 2, \dots, N$):

$$\ddot{x}_i = c_i. \quad (7)$$

Note that the control law (6) has achieved two objectives: (a) it has linearized the input-output behavior of the i th vehicle's dynamics; and (b) it has resulted in dynamics, for each vehicle, which are independent of the vehicle's particular characteristics (e.g., mass of the vehicle, engine time lag, etc.).

Fig. 2. Linearized model of the i th vehicle with control input c_i , $i = 1, 2, \dots, N$.

C. Control Laws

We propose the following linear control laws for the linearized vehicle model (7): for the first linearized vehicle model the control law is

$$c_1 := c_p \Delta_1(t) + c_v \dot{\Delta}_1(t) + c_a \ddot{\Delta}_1(t) + k_v [v_l(t) - v_l(0-)] + k_a a_l(t) \quad (8)$$

where $v_l(0-)$ denotes the steady-state value of the lead vehicle's velocity (v_l) (the first vehicle can calculate v_l and a_l from v_1 , a_1 , $\dot{\Delta}_1$ and $\ddot{\Delta}_1$). For the i th linearized vehicle model ($i = 2, 3, \dots, N$) the control law is

$$c_i := c_p \Delta_i(t) + c_v \dot{\Delta}_i(t) + c_a \ddot{\Delta}_i(t) + k_v [v_{i-1}(t) - v_{i-1}(0-)] + k_a a_{i-1}(t) \quad (9)$$

where $v_{i-1}(0-)$ denotes the steady-state value of the $i-1$ th vehicle's velocity and c_p , c_v , c_a , k_v , and k_a are design constants. Fig. 2 shows the linearized model of the i th vehicle with the proposed control laws c_i .

D. Platoon Dynamics

Let $w_l(t)$ denote the deviation of the lead vehicle's velocity from its steady-state value at time t (i.e., $w_l(t) := v_l(t) - v_l(0-)$). Then, using the proposed control laws (8)–(9) for

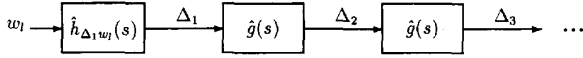


Fig. 3. Block diagram for a platoon of linearized vehicle models.

the linearized vehicle models, we obtain the block diagram in Fig. 3 where:

$$\hat{h}_{\Delta_1 w_l}(s) := \frac{s^2 - k_a s - k_v}{s^3 + c_a s^2 + c_v s + c_p} \quad (10)$$

and for $i = 2, 3, \dots, N$

$$\hat{g}(s) := \hat{h}_{\Delta_i \Delta_{i-1}}(s) = \frac{(c_a + k_a)s^2 + (c_v + k_v)s + c_p}{s^3 + c_a s^2 + c_v s + c_p}. \quad (11)$$

In (10) and (11) we have used the symbol “ $\hat{\cdot}$ ” to distinguish Laplace transforms from the corresponding time-domain functions. Thus $\hat{h}_{ab}(\cdot)$ denotes the transfer function from b to a .

In the next section, we use the block diagram in Fig. 3 to analyze the platoon dynamics.

III. DESIGN OF THE PROPOSED CONTROL LAWS

In this section, we discuss the main design objectives for the longitudinal control laws and propose a design by solving a constrained optimization problem.

A. Design Considerations

Some consideration of Fig. 3 suggests the main design objectives for the longitudinal control laws:

- 1) Stability requires the $\hat{h}_{\Delta_1 w_l}$ and \hat{g} have all their poles in the open left half-plane of the s -plane.
- 2) $\hat{h}_{\Delta_1 w_l}$ should be designed so that the deviation of the first vehicle from its assigned position (i.e., Δ_1) remains small as a result of the change in the velocity of the lead vehicle (w_l); in addition, it is desirable to have the deviation of the i th vehicle (for $i = 1, 2, \dots, N$) asymptotically approach zero (i.e., $\Delta_i(t) \rightarrow 0$ as $t \rightarrow \infty$), at the end of a maneuver.
- 3) Since the magnitude of Δ_i (for $i = 1, 2, \dots, N$) due to changes (w_l) in the lead vehicle's velocity from its steady-state value should not increase from one vehicle to the next as one goes down the platoon, we require the $|\hat{g}(j\omega)| < 1$ for all $\omega > 0$, (to avoid a slinky-type effect).
- 4) Since the inverse Laplace transform of $[\hat{g}(s)]^2$ is the convolution of the impulse response of $\hat{g}(s)$ with itself (i.e., $g * g(t)$), to avoid oscillatory behavior down the platoon it is desirable to have $g(t) > 0$ for all $t > 0$.

From Fig. 3, we note that for $i = 1, 2, \dots, N$

$$\hat{\Delta}_i(s) = \hat{h}_{\Delta_1 w_l}(s) [\hat{g}(s)]^{i-1} \hat{w}_l(s). \quad (12)$$

Suppose the lead vehicle reaches its final steady-state value at time t_f . We can write: for $t > 0$,

$$w_l(t) = [v_l(t_f) - v_l(0-)] + \tilde{w}_l(t) \quad (13)$$

where $\tilde{w}_l(t) = 0$ for all $t > t_f$.

Taking Laplace transforms of both sides of (13) we obtain

$$\hat{w}_l(s) = \frac{v_l(t_f) - v_l(0-)}{s} + \hat{\tilde{w}}_l(s). \quad (14)$$

Substituting (14) into (12) and using the final value theorem, we obtain (for $i = 1, 2, \dots, N$)

$$\lim_{t \rightarrow \infty} \Delta_i(t) = \lim_{s \rightarrow 0} s \hat{\Delta}_i(s) = \lim_{s \rightarrow 0} s \hat{h}_{\Delta_1 w_l}(s) [\hat{g}(s)]^{i-1} \cdot \left[\frac{v_l(t_f) - v_l(0-)}{s} + \hat{\tilde{w}}_l(s) \right]. \quad (15)$$

Since $\hat{g}(0) = 1$ from (11) and $\hat{\tilde{w}}_l(0) = \int_0^{t_f} \tilde{w}_l(t) dt > 0$, from (15) we obtain (for $i = 1, 2, \dots, N$)

$$\lim_{t \rightarrow \infty} \Delta_i(t) = \hat{h}_{\Delta_1 w_l}(0) [v_l(t_f) - v_l(0-)]. \quad (16)$$

We choose $k_v = 0$ so that from (10) and (16) we obtain $\lim_{t \rightarrow \infty} \Delta_i(t) = 0$ for $i = 1, 2, \dots, N$.

B. Design of $\hat{h}_{\Delta_1 w_l}$ and \hat{g}

Having chosen $k_v = 0$, we still need to design parameters k_a , c_a , c_v , and c_p . We choose the design vector (q) as follows

$$q := [\alpha, \beta, p, k_a]^T \quad (17)$$

where

$$\begin{aligned} c_a &= -\alpha - p \\ c_v &= \alpha p + \beta \\ c_p &= -\beta p. \end{aligned} \quad (18)$$

From (10), (11), and (18), we write the design transfer functions as follows:

$$\hat{h}_{\Delta_1 w_l}(s, q) = \frac{s^2 - k_a s}{(s^2 - \alpha s + \beta)(s - p)} \quad (19)$$

$$\hat{g}(s, q) = \frac{(-\alpha - p + k_a)s^2 + (\alpha p + \beta)s - \beta p}{(s^2 - \alpha s + \beta)(s - p)}. \quad (20)$$

From (19) and (20) we note that

$$s \hat{h}_{\Delta_1 w_l}(s, q) + \hat{g}(s, q) = 1 \quad (21)$$

for all $s \in C$ and for all $q \in R^4$; hence, we cannot design $\hat{h}_{\Delta_1 w_l}(s, q)$ and $\hat{g}(s, q)$ independently. Thus we choose target transfer functions

$$\hat{h}_{\text{target}}(s) = \frac{s^2}{(s+4)(s+5)(s+6)} \quad (22)$$

$$\hat{g}_{\text{target}}(s) = \frac{5s^2 + 49s + 120}{(s+4)(s+5)(s+6)} \quad (23)$$

which are based on the design considerations above and on our work in [11], [12]. Next, we formulate a design strategy by solving an optimization problem.

C. Optimization Problem

We choose to compute the solution q^* of the following problem:

$$\min_{q \in R_s^4} f^0(q) \quad (24)$$

where $R_s^4 := \{q \in R^4 | \hat{h}_{\Delta_1 w_l}(s, q) \text{ and } \hat{g}(s, q) \text{ stable transfer functions}\}$ and

$$f^0(q) := \sum_{k=1}^n w_k^h \left[|\hat{h}_{\Delta_1 w_l}(j\omega_k, q)|^2 - |\hat{h}_{\text{target}}(j\omega_k)|^2 \right] + \sum_{k=1}^n w_k^g \left[|\hat{g}(j\omega_k, q)|^2 - |\hat{g}_{\text{target}}(j\omega_k)|^2 \right]. \quad (25)$$

Equation (25) represents a weighted quadratic cost function with w_k^h and w_k^g (for $k = 1, 2, \dots, n$) denoting the appropriate weights and n chosen appropriately to include all frequencies of interest. Since most of the energy of $w_l(\cdot)$ is between 0 rad/s and 3 rad/s, w_k^h and w_k^g (for ω_k between these frequencies) were chosen to be much larger than the corresponding weights (w_k^h and w_k^g) for frequencies between 3 rad/s and 6 rad/s. To decrease the effect of higher frequency signals on the designed control laws, w_k^h and w_k^g (for ω_k greater than 6 rad/s) were chosen large enough so that the magnitude of the frequency response of the designed transfer functions closely approximated the corresponding magnitude of the frequency response of the target transfer functions.

To compute the minimizer q^* to the contained optimization problem (24) we use a gradient descent algorithm *similar* to Armijo's gradient algorithm [1]:

- **Initial Data:** $\gamma \in (0, 1)$
- **Step 0:** $i = 0$; $q_0 = [-9, 20, -6, -3]^T$
- **Step 1:** Compute the search direction $h_i := h(q_i) := -\nabla f^0(q_i)$; stop if $\nabla f^0(q_i) = 0$.
- **Step 2:** Compute the largest $\mu_i \in (0, 1)$ such that a) $\hat{h}_{\Delta_1 w_l}(s, q_i - \mu_i \nabla f^0(q_i))$ and $\hat{g}(s, q_i - \mu_i \nabla f^0(q_i))$ are stable transfer functions and b) their poles and the zeros of $\hat{h}_{\Delta_1 w_l}(s, q_i - \mu_i \nabla f^0(q_i))$ have not moved by more than 0.1 with respect to their respective poles and zeros locations in $\hat{h}_{\Delta_1 w_l}(s, q_i)$ and $\hat{g}(s, q_i)$.
- **Step 3:** Compute the step size $\mu_i^{k_i} := \arg\max \{\mu_i^k : f^0(q_i - \mu_i^k \nabla f^0(q_i)) - f^0(q_i) \leq -\mu_i^k \gamma \|\nabla f^0(q_i)\|^2\}$ (k_i is the least integer $k \geq 1$ such that the condition is satisfied) and set

$$\lambda_i := \mu_i^{k_i}$$

- **Step 4:** Update

$$q_{i+1} = q_i + \lambda_i h_i$$

$i \rightarrow i + 1$ and go to Step 1.

The above optimization algorithm differs from the standard Armijo algorithm in Step 2, in that stability of $\hat{h}_{\Delta_1 w_l}$ and \hat{g} requires that at the i th iteration, we compute the largest step size $\mu_i \in (0, 1)$ so that $\hat{h}_{\Delta_1 w_l}(s, q_i - \mu_i \nabla f^0(q_i))$ and $\hat{g}(s, q_i - \mu_i \nabla f^0(q_i))$ are stable transfer functions.

In the above algorithm, we approximated $\nabla f^0(\cdot)$ as follows: denote the k th entry of $\nabla f^0(\cdot)$ by $\nabla f_k^0(\cdot)$ (for $k = 1, \dots, 4$).

$$\Delta f_k^0(q) \approx \frac{f^0(q + \epsilon e_k) - f^0(q)}{\epsilon} \quad (26)$$

where $e_k \in R^4$ denotes the unit vector with a 1 in the k th entry and a zero in every other entry and $\epsilon = 10^{-4}$. The stopping rule in Step 1 was implemented as follows: stop if $\nabla f^0(q_i) < 10^{-6}$.

Using the above algorithm, we obtain the following final design transfer functions:

$$\hat{h}_{\text{final}}(s) = \frac{s^2 + 5.15s}{(s + 1.71)(s + 4.93)(s + 10.92)} \quad (27)$$

$$\hat{g}_{\text{final}}(s) = \frac{12.42s^2 + 80.96s + 91.99}{(s + 1.71)(s + 4.93)(s + 10.92)}. \quad (28)$$

The corresponding values of the design variables are

$$[c_p, c_v, c_a, k_v, k_a] = [91.99, 80.96, 17.56, 0, -5.15]. \quad (29)$$

Denote $\hat{h}_{\text{initial}} := \hat{h}_{\Delta_1 w_l}(s, q_0)$ and $\hat{g}_{\text{initial}}(s) := \hat{g}(s, q_0)$ where q_0 is the initial design vector in Step 0 of the optimization algorithm. Figs. 4 and 6 show the magnitudes of frequency response of $\omega \mapsto \hat{h}_{\text{initial}}(j\omega)$, $\omega \mapsto \hat{h}_{\text{final}}(j\omega)$, $\omega \mapsto \hat{h}_{\text{target}}(j\omega)$, $\omega \mapsto \hat{g}_{\text{initial}}(j\omega)$, $\omega \mapsto \hat{g}_{\text{final}}(j\omega)$, and $\omega \mapsto \hat{g}_{\text{target}}(j\omega)$. The corresponding impulse responses are shown in Figs. 5 and 7.

IV. SIMULATION RESULTS

To examine the performance of (8)–(9) with the design constants (29), we ran simulations for platoons consisting of three different types of vehicles. Within each platoon, 15 vehicles ($N = 15$) followed a lead vehicle. In all the simulations conducted, all the vehicles are assumed to be traveling initially at the steady-state velocity of $v_0 = 17.9$ m/s (i.e., 40 mph). Beginning at time $t = 0$ s, the lead vehicle's velocity increases from its steady-state value of 17.9 m/s until it reaches its final value of 21.9 m/s (i.e., 50 mph); the maximum jerk and the peak acceleration values corresponding to this velocity time-profile were 0.5 m/s³ and 1 m/s², respectively (see Figs. 8 and 9).

Figs. 10 and 11 show the simulations results for the nominal case:

- The deviations of the vehicles from their assigned positions (i.e., Δ_i for $i = 1, 2, \dots, 15$) are less than 0.08 m.
- These deviations decrease to zero reasonably fast and do not exhibit too much oscillatory behavior.
- The peak values of these deviations *increase* from one vehicle to the next as one goes down the platoon. This is due to the fact that $|\hat{g}_{\text{final}}(j\omega)| \geq 1$ for ω between 0 rad/s and 6 rad/s.
- The acceleration curves show that the peak magnitude of vehicle accelerations increases from one vehicle to the next as one goes down the platoon. The peak values of these accelerations remain within 1.5 m/s².

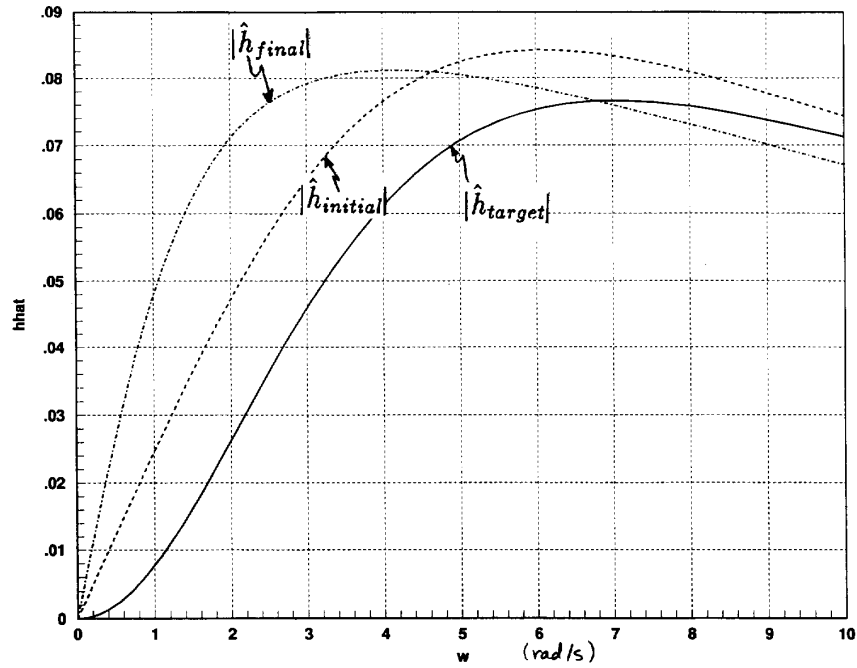


Fig. 4. $|\hat{h}_{\text{initial}}(jw)|$, $|\hat{h}_{\text{final}}(jw)|$, and $|\hat{h}_{\text{target}}(jw)|$ versus w .

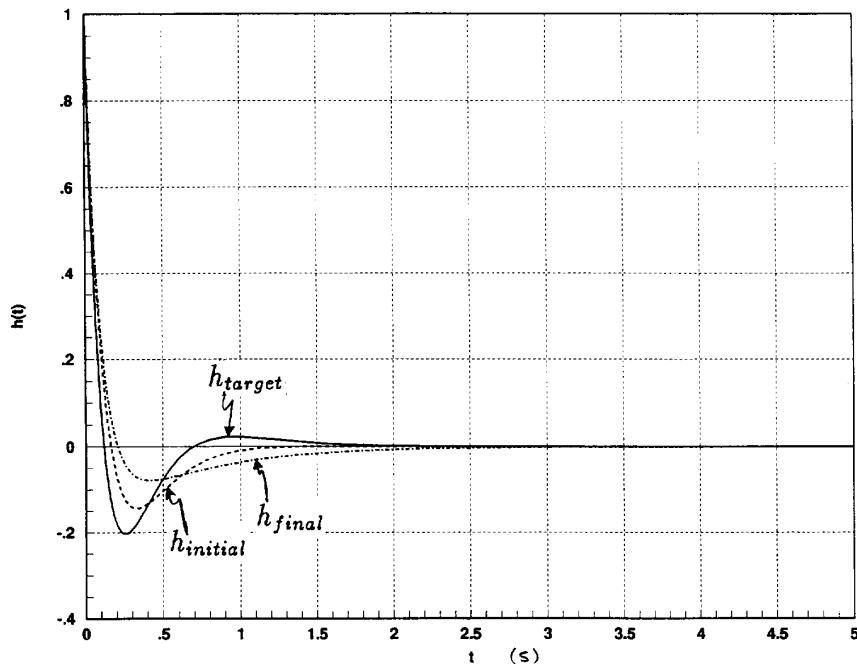


Fig. 5. $h_{\text{initial}}(t)$, $h_{\text{final}}(t)$, and $h_{\text{target}}(t)$ versus t .

In comparison to [11], [12], the peak value of the lead vehicle's acceleration (a_l) is 1 m/s^2 ; whereas in [11], [12], this peak value was 3 m/s^2 . The maneuver considered here was chosen to be gentler because otherwise the acceleration

demands on the tail vehicle of the platoon were excessive.

In contrast to [11], [12], the deviations of the vehicles from their assigned positions (i.e., Δ_i for $i = 1, 2, \dots, 15$)

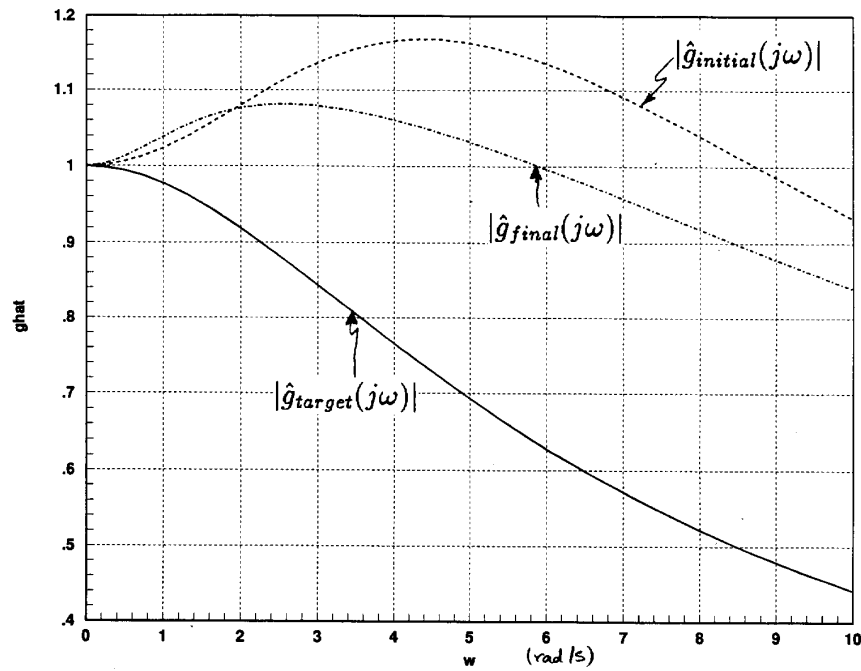


Fig. 6. $\hat{g}_{\text{initial}}(jw)$, $\hat{g}_{\text{final}}(jw)$, and $\hat{g}_{\text{target}}(jw)$ versus w .

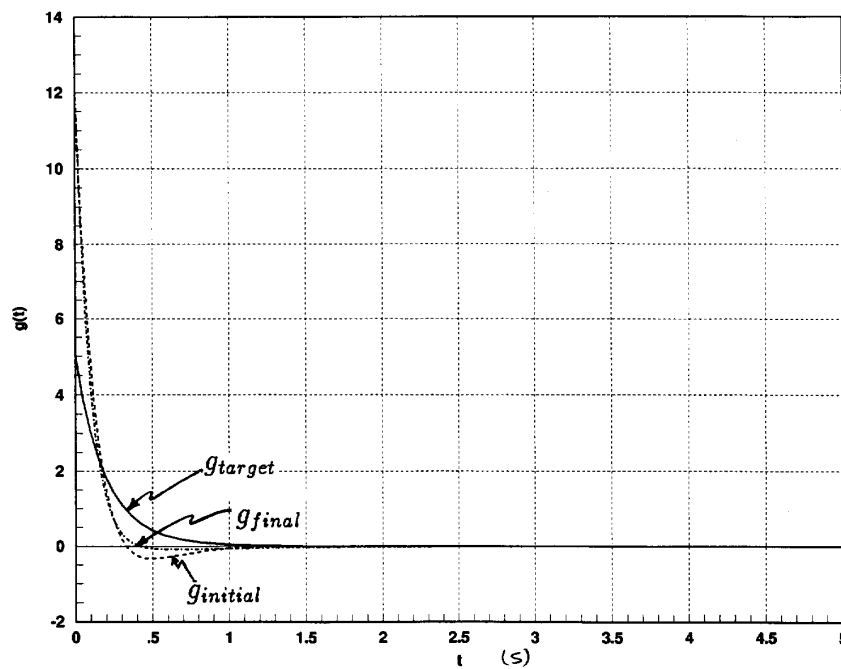


Fig. 7. $g_{\text{initial}}(t)$, $g_{\text{final}}(t)$, and $g_{\text{target}}(t)$ versus t .

increase from one vehicle to the next under the control laws (8)–(9); however, the peak values of these deviations are within acceptable performance limits, and these deviations do not exhibit too much oscillatory behavior.

Since under the control laws (8)–(9), the i th vehicle in the platoon (for $i = 2, 3, \dots, 15$) does not require the lead vehicle's velocity (v_l) and acceleration (a_l) for computing its control input (c_i), the longitudinal control scheme presented

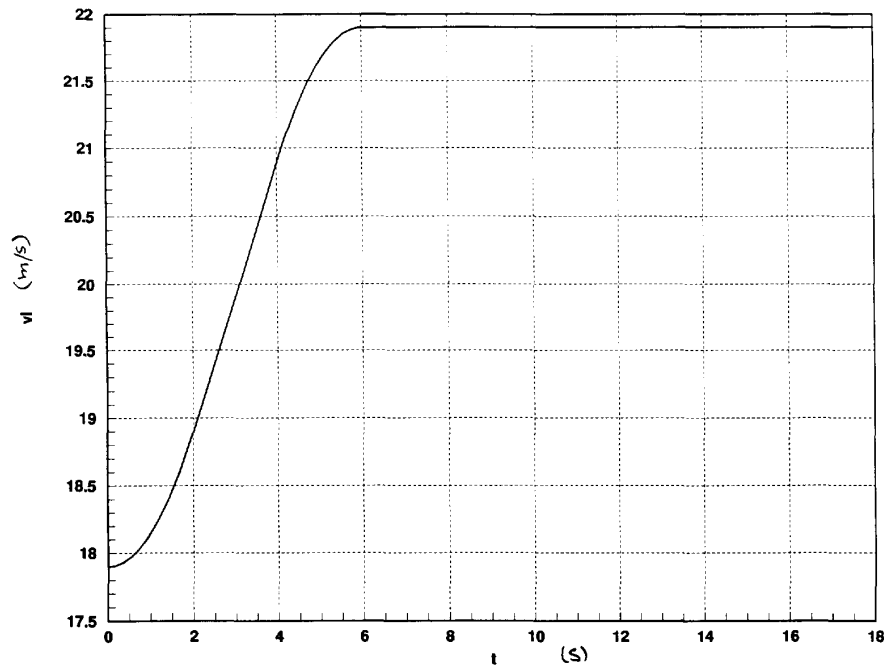


Fig. 8. Lead vehicle's velocity time profile: $v_l(t)$ versus t .

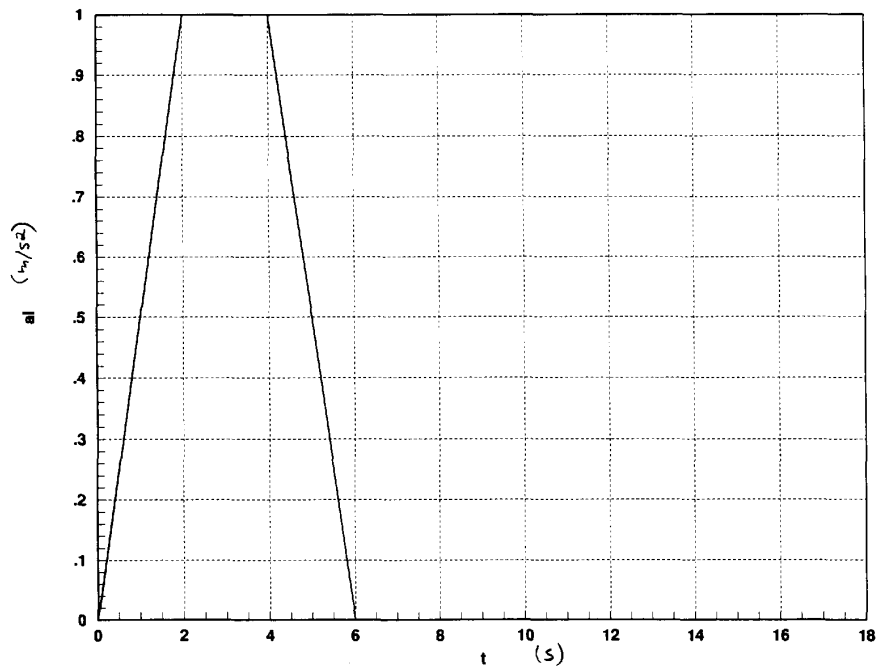


Fig. 9. Lead vehicle's acceleration time profile: $a_l(t)$ versus t .

here does not necessitate a communication system; hence, the implementation of this longitudinal control scheme is less expensive than the one presented in [11], [12]. The performance of the longitudinal control scheme in [11], [12] degrades slightly due to communication delays in transmitting the lead vehicle information; in contrast, control laws (8)–(9)

do not depend on transmission of the lead vehicle information to each vehicle in the platoon.

The linearization method is based on exact knowledge of vehicle/engine parameters. We ran simulations to evaluate the robustness of the control laws (8)–(9) with the design constants (29); namely, robustness with respect to each vehicle's mass

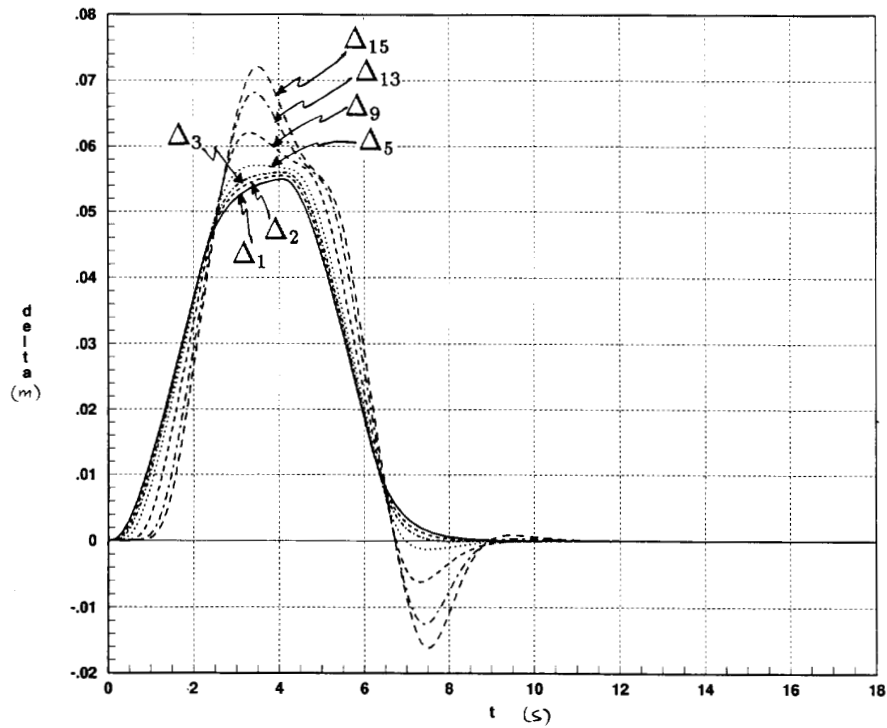


Fig. 10. $\Delta_1, \Delta_2, \Delta_3, \Delta_5, \Delta_9, \Delta_{13}$, and Δ_{15} versus t : nominal case.

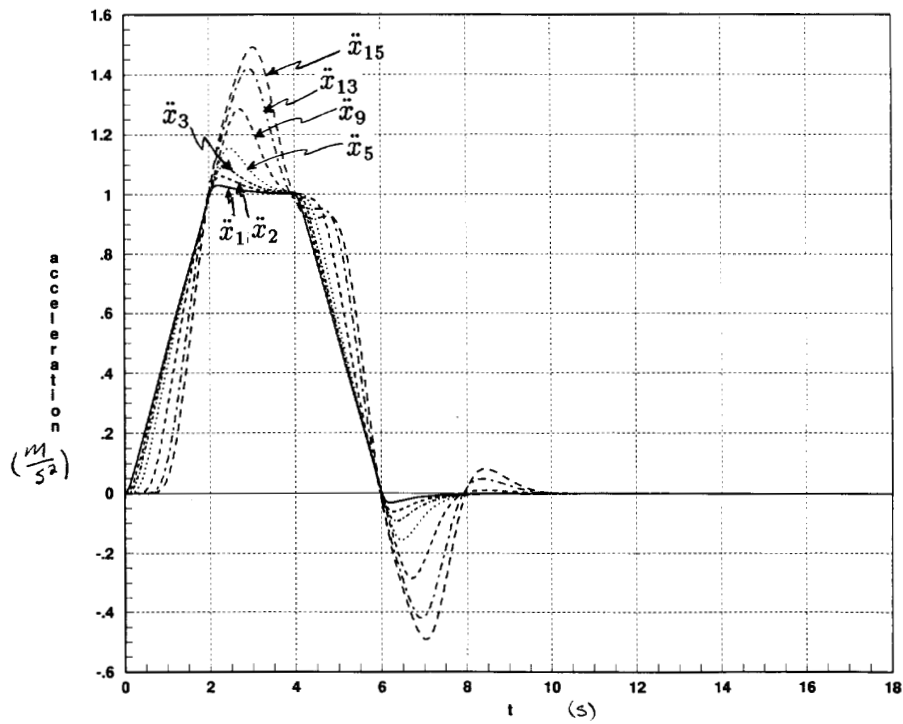


Fig. 11. $\ddot{x}_1, \ddot{x}_2, \ddot{x}_3, \ddot{x}_5, \ddot{x}_9, \ddot{x}_{13}$, and \ddot{x}_{15} versus t : nominal case.

variations and measurement noise. The mass variations ranged (for $i = 1, 2, \dots, 15$) used in the i th vehicle's control laws from 8 to 23% of each vehicle's mass. The value of Δ_i (8)–(9) was the sum of the actual measured value of Δ_i and

some Gaussian noise with zero mean and standard deviation (σ) of 0.05 m. Based on these simulations, the deviations of the vehicles from their respective positions were larger than the respective deviations in the nominal case; however, such deviations were within acceptable performance limits.

V. CONCLUSION

In contrast to previous work [11], [12] this paper considers longitudinal control laws for a platoon of vehicles which do not use any communication of lead vehicle information.

Comparison with a full communication case [11], [12] shows that when using control laws (8)–(9), the deviations in vehicle spacings from their assigned positions increase from one vehicle to the next as one goes down the platoon. Furthermore, the acceleration demands on the tail vehicle of the platoon are much larger than the respective demands under the control laws in [11], [12]. On the other hand, the longitudinal control scheme presented here does not require communication of lead vehicle information; hence, it is less expensive than the corresponding scheme in [11], [12] and cannot suffer from any degradation due to communication delays. The present work is a preliminary study; it does show that loss of communication implies a loss of performance.

At present system designers are inclined to view the communication system within the platoon to be indispensable for safety, entrainment, and detrainment maneuvers. This study shows that if communications breaks down, the control laws proposed in this paper can be used as alternative means to control the longitudinal dynamics of a platoon of vehicles.

REFERENCES

- [1] L. Armijo, "Minimization of functions having Lipschitz continuous first partial derivatives," *Pacific J. Mathematics*, vol. 16, pp. 1–3, 1966.
- [2] R. J. Caudill and W. L. Garrard, "Vehicle-follower longitudinal control for automated transit vehicles," *ASME J. Dynamic Syst., Meas. Contr.*, vol. 99, no. 4, pp. 241–248, Dec. 1977.
- [3] H. Y. Chiu, G. B. Stupp, Jr., and S. J. Brown, Jr., "Vehicle-follower control with variable gains for short headway automated guideway transit systems," *ASME J. Dynamic Syst., Meas. Contr.*, vol. 99, no. 3, pp. 183–189, Sept. 1977.
- [4] A. S. Hauksdottir and R. E. Fenton, "On the design of a vehicle longitudinal control," *IEEE Trans. Veh. Technol.*, vol. VT-34, pp. 182–187, Nov. 1985.
- [5] A. S. Hauksdottir and R. E. Fenton, "On vehicle longitudinal controller design," in *Proc. 1988 IEEE Workshop Automotive Applications Electron.*, pp. 77–83, 1988.
- [6] A. Hitchcock, private communication at Univ. Calif. Berkeley, Inst. Transportation Studies, 1990.
- [7] L. L. Hoberock and R. J. Rouse, Jr., "Emergence control of vehicle platoons systems operation and platoon leader control," *ASME Dynamic Syst. Meas. Contr.*, vol. 98, no. 3, pp. 245–251, Sept. 1976.
- [8] A. Isidori, *Nonlinear Control Systems*, 2nd ed. Springer-Verlag, 1989.
- [9] R. J. Rouse, Jr. and L. L. Hoberock, "Emergency control of vehicle platoons: control of following-law vehicles," *ASME J. Dynamic Syst., Meas. Contr.*, vol. 98, no. 3, pp. 239–244, Sept. 1976.
- [10] S. S. Sastry and A. Isidori, "Adaptive control of linearizable systems," *IEEE Trans. Automat. Contr.*, vol. 34, pp. 1123–1131, Nov. 1989.
- [11] S. Sheikholeslam and C. A. Desoer, "A system level study of the longitudinal control of a platoon of vehicles," *ASME J. Dynamic Syst., Meas. Contr.*, vol. 114, no. 2, pp. 286–292, June 1992.
- [12] S. Sheikholeslam and C. A. Desoer, "Longitudinal control of a platoon of vehicles," in *Proc. American Contr. Conf.*, vol. 1, pp. 291–297, May 1990.
- [13] S. Sheikholeslam and C. A. Desoer, "Longitudinal control of a platoon of vehicles with no communication of lead vehicle information," in *Proc. American Contr. Conf.*, vol. 3, pp. 3102–3107, June 1991.
- [14] S. E. Shladover, "Operation of automated guideway transit vehicles in dynamically reconfigured trains and platoons," presented at *Automated Guideway Transit Technology Program*, UMTA-MA-06-00855-79-1, April 1979.
- [15] S. E. Shladover, "Longitudinal control of automotive vehicles in close-formation platoons," *ASME J. Dynamic Syst. Meas. Contr.*, vol. 113, no. 2, pp. 231–241, June 1991.
- [16] S. Shladover, C. A. Desoer, J. K. Hedrick, M. Tomizuka, J. Walrand, W. B. Zhang, D. McMahon, H. Peng, S. Sheikholeslam, and N. McKeown, "Automatic vehicle control developments in the PATH program," *IEEE Trans. Veh. Technol.*, vol. 40, pp. 114–130, Feb. 1991.
- [17] G. M. Takasaki and R. E. Fenton, "On the identification of vehicle longitudinal dynamics," *IEEE Trans. Automat. Contr.*, vol. 22, pp. 610–615, Aug. 1977.



Shahab Sheikholeslam (S'87–M'92) received the B.S. degree in computer engineering and the B.A. degree in mathematics from the University of California, Santa Cruz, in 1988, the M.S. degree in electrical engineering from the University of California, Berkeley, in 1989, and the Ph.D. degree in 1991 from the Department of Electrical Engineering and Computer Sciences at the University of California, Berkeley.

He is currently with Measurex Corporation, Cupertino, CA. His research interests include nonlinear and adaptive control, and decentralized control of interconnected nonlinear dynamical systems and process control application.

Dr. Sheikholeslam is a member of Phi Beta Kappa.



Charles A. Desoer (S'50–A'53–SM'57–F'64–LF'92) received the Sc.D. degree from the Massachusetts Institute of Technology in 1953.

He worked at the Bell Telephone Laboratories, Murray Hill, from 1953 to 1958. From 1958 to the present, he has worked in the Department of Electrical Engineering and Computer Sciences at the University of California at Berkeley. From 1967 to 1968, he was at the Miller Institute. His research interests are in system theory, control systems, and circuits. He has co-authored several books, including *Feedback Systems: Input-Output Properties* (1975, with M. Vidyasagar); *Multi-variable Feedback Systems* (1982, with F. M. Callier); *Linear and Nonlinear Circuits* (1987, with L. O. Chua and E. S. Kuh); *Algebraic Theory of Linear Feedback Systems with Full and Decentralized Compensators* (1990, with A. N. Gunders); and *Linear System Theory* (1991, with F. M. Callier). Dr. Desoer received the Guggenheim Fellowship in 1970 to 1971; the IEEE Education Medal and the Prix Montefiore in 1975; the American Automatic Control Education Award in 1983; and the IEEE Control Systems Science and Engineering Award in 1986. He is a member of the National Academy of Engineering.